AIMS Mathematics, 11(3): 7779–7790.
DOI: 10.3934/math.2026320
Received: 27 December 2025
Revised: 16 February 2026
Accepted: 17 March 2026
Published: 24 March 2026

https://www.aimspress.com/journal/Math

Research article

Asymptotic modelling of spherical particle dissolution under a uniform flow

Awatif Alhowaity*

Department of Mathematics, Applied College in Alkamil, University of Jeddah, Jeddah, Saudi Arabia

* **Correspondence:** Email: asalhowaity@uj.edu.sa.

Abstract: The dissolution of solid particles in liquids is commonly modeled as a diffusion-controlled process coupled with a moving boundary. While such models allow for analytical solutions under stationary conditions, they do not account for the effects of fluid motion that commonly arise in practical situations. In the present work, this classical model is extended by incorporating advective transport due to an imposed uniform flow. The dissolution process is formulated as a free boundary problem governed by an advection-diffusion equation in the exterior of the particle, coupled with a Stefan-type condition describing the interface motion. By introducing a non-dimensionalization, the problem is characterized by the Péclet number, which measures the relative importance of advection and diffusion. An asymptotic expansion in the Péclet number is employed to develop semi-analytical asymptotic solutions. The leading-order term recovers the diffusion controlled self-similar behavior, while higher-order corrections reveal how uniform flow modifies the concentration field and increases the dissolution rate. In particular, it is shown that the first non-zero flow-induced correction to the interface motion arises at second order, reflecting the inherently nonlinear nature of advection effects. The analysis provides a mathematically consistent extension of diffusion-only dissolution models and offers new insight into flow-induced dissolution mechanisms.

Keywords: spherical particle dissolution; advection diffusion equation; free boundary problem; Stefan condition; asymptotic analysis; uniform flow; moving boundary
Mathematics Subject Classification: 35K05, 35R35, 76R50

1. Introduction

The dissolution of solid particles in liquids is a fundamental transport process that arises in a wide range of physical and engineering applications, including phase change phenomena, materials processing, and chemical transport. From a mathematical perspective, particle dissolution is commonly described as a diffusion-driven mass transfer process coupled with the motion of a dissolving interface. This coupling naturally gives rise to free boundary problems of Stefan type, which have been

extensively studied in the context of diffusion-controlled phase change and dissolution processes [1–3].

In diffusion-controlled settings, where the surrounding fluid is assumed to be quiescent, the governing equations often admit self-similar analytical solutions. Such solutions provide valuable insight into the dissolution dynamics and the temporal evolution of the particle radius [2]. Analytical formulations for spherical particle dissolution in stationary fluids show that the concentration field remains purely radial and that the particle radius decreases proportionally to the square root of time [2, 4]. A recent analytical study by the author established a diffusion-dominated framework for spherical particle dissolution with a moving boundary and derived an explicit Stefan condition governing the interface motion [5].

Despite their analytical tractability, diffusion-only models have limited applicability in situations where fluid motion is present. In many practical environments, dissolved material is transported away from the particle surface by flow, thereby modifying local concentration gradients and altering the dissolution rate. From a mathematical standpoint, the introduction of fluid motion adds an advective transport mechanism to the governing equations, leading to advection-diffusion formulations that break radial symmetry and invalidate the classical self-similar structure underlying diffusion-controlled solutions [6]. While advective transport has been investigated in related mass-transfer problems, fully analytical treatments of moving-boundary dissolution in the presence of flow remain relatively limited.

To address this limitation, the dissolution process is examined in the presence of an imposed uniform flow by coupling advective transport with diffusion in a free boundary model. The concentration field in the liquid phase is governed by an advection-diffusion equation in the exterior of the particle, together with a Stefan-type condition describing the interface motion. The relative importance of advection and diffusion is characterized by the number Péclet. An asymptotic expansion in this parameter allows the influence of flow on both the concentration field and the interface evolution to be quantified systematically. By employing an asymptotic expansion in the Péclet number, the effect of flow on both the concentration field and the interface evolution is quantified in a systematic manner [7]. The analysis shows that uniform flow generates anisotropic corrections to the concentration field at first order, while the first non-zero modification of the dissolution rate arises only at second order. This behavior reflects the inherently nonlinear nature of flow-induced effects and provides a mathematically consistent extension of diffusion-controlled dissolution models. Recent advances in the study of non-Newtonian fluids, particularly Maxwell fluids and hybrid nanofluids, have provided valuable insights into complex transport phenomena in industrial and biomedical applications [8–10]. These studies demonstrate the significance of understanding fluid rheology in transport processes, which motivates the present investigation of dissolution dynamics in a flowing environment.

2. Mathematical formulation

We consider a solid spherical particle of radius $S(t)$ immersed in an incompressible Newtonian fluid. The particle dissolves over time, releasing a soluble species into the surrounding liquid. The concentration field of the dissolved substance, denoted by $C(\mathbf{x}, t)$, is governed by an advection diffusion equation in the exterior domain $r > S(t)$. The flow is assumed to be a prescribed uniform stream of velocity U in the positive z-direction. This approximation is justified for small Péclet numbers and short times, because the hydrodynamic disturbance generated by the slowly shrinking particle remains negligible compared to the dominant diffusive transport [2, 3].

The problem is formulated in spherical coordinates (r, θ, ϕ) with origin at the centre of the particle. By symmetry, all quantities are independent of the azimuthal angle ϕ. The particle radius evolves according to the Stefan condition, which expresses mass conservation at the moving interface.

2.1. Governing equations

The dimensionless form of the equations is obtained by scaling lengths with the initial radius S_0, time with the diffusion scale S_0^2/D, and concentration with $C_p - C_0$ (the difference between the particle solubility and the far-field concentration). The dimensionless concentration is therefore defined as

$$c = \frac{C - C_0}{C_p - C_0}.$$

In the fluid region $r > S(t)$, the concentration satisfies

$$\frac{\partial c}{\partial t} + \mathrm{Pe}\,\frac{\partial c}{\partial z} = \nabla^2 c, \qquad r > S(t), \tag{2.1}$$

where the Péclet number

$$\mathrm{Pe} = \frac{US_0}{D} \tag{2.2}$$

measures the relative importance of advection and diffusion. The operator ∇^2 denotes the Laplacian in spherical coordinates. Because the imposed velocity is uniform and directed along the z-axis, $\mathbf{u} = U\hat{\mathbf{z}}$, and the advective term simplifies to $\partial c/\partial z$.

At the particle surface, the concentration is maintained at the saturation value,

$$c = 1 \quad \text{on } r = S(t), \tag{2.3}$$

and far from the particle,

$$c \to 0 \quad \text{as } r \to \infty. \tag{2.4}$$

2.2. Stefan condition

Mass conservation at the moving interface requires that the net mass flux leaving the solid equals the diffusive flux into the liquid. With the outward normal pointing radially outward, the dimensional Stefan condition is written as

$$(C_s - C_p)\,\frac{dS}{dt} = -D\,\frac{\partial C}{\partial r}\Big|_{r=S},$$

where the minus sign ensures consistency of flux orientation during dissolution.

We now introduce the dimensionless parameter

$$\beta = \frac{C_p - C_0}{C_s - C_p}, \tag{2.5}$$

which is positive because $C_s > C_p > C_0$. This definition is chosen so that the final expression for the dissolution constant k takes a compact form when the short-time similarity solution is developed.

Using (2.5), we have $C_s - C_p = (C_p - C_0)/\beta$, and substituting into the dimensional Stefan condition gives

$$\frac{C_p - C_0}{\beta}\,\frac{dS}{dt} = -D\,\frac{\partial C}{\partial r}\Big|_{r=S}.$$

Dividing by $C_p - C_0$ and introducing the dimensionless variables yields the non-dimensional Stefan condition

$$-\frac{1}{\beta}\frac{dS}{dt} = \left.\frac{\partial c}{\partial r}\right|_{r=S(t)}. \tag{2.6}$$

For a dissolving particle $dS/dt < 0$, the left-hand side of (2.6) is positive. Equation (2.6) expresses the conservation of solute mass at the moving interface, with the sign convention chosen to be consistent with the outward normal and the planar similarity mapping introduced in Section 3.

2.3. Initial conditions

The problem is closed by specifying the initial state. At $t = 0$, the particle has unit radius and the surrounding fluid is completely free of solute:

$$S(0) = 1, \qquad c(r, \theta, 0) = 0 \quad \text{for } r > 1. \tag{2.7}$$

2.4. Remarks on the flow model

The uniform velocity field $\mathbf{u} = U\hat{\mathbf{z}}$ is prescribed without solving the full hydrodynamic problem. This simplification is legitimate under the assumptions of the asymptotic analysis: we consider only the early stages of dissolution ($\sqrt{t} \ll 1$) and small Péclet numbers (Pe $\ll 1$). In this regime, the diffusion layer remains thin, and the momentum boundary layer (where the no-slip condition would be felt) is either thick compared to the concentration layer (high Schmidt number) or its influence on the leading-order mass transfer is subordinate to diffusive transport [6, 11]. A more realistic Stokes-flow disturbance would modify the details of the O(Pe) correction, but the essential qualitative features, the dipolar symmetry of the first-order concentration field and the vanishing of its angular average, are expected to persist. The uniform-flow approximation should be interpreted as a far-field model valid outside the thin hydrodynamic boundary layer, whose detailed structure does not affect the leading-order mass transfer in the regime considered. The present model therefore captures the leading effects of a weak uniform flow on the dissolution kinetics in a mathematically tractable manner.

3. Solution of the problem

3.1. Short-time planar approximation

We focus on the early stage of dissolution, during which the diffusion length $\sqrt{t}$ remains small compared to the initial particle radius (scaled to unity). In this regime, the curvature of the spherical interface has a subleading effect in the thin diffusive boundary layer adjacent to the surface. Consequently, the radial operator can be approximated locally by its planar counterpart [7].

The external flow is assumed to remain uniform and unaffected by the slow shrinkage of the particle. This assumption is justified for small Péclet numbers and short times, where hydrodynamic disturbances generated by the moving boundary remain negligible compared to diffusive transport.

We introduce the planar similarity variable

$$\xi = \frac{1 - r}{\sqrt{t}}, \qquad S(t) = 1 - k\sqrt{t}, \qquad k > 0. \tag{3.1}$$

The interface velocity satisfies

$$\frac{dS}{dt} = -\frac{k}{2\sqrt{t}} < 0, \tag{3.2}$$

which corresponds to a monotonically shrinking particle.

The initial conditions are

$$S(0) = 1, \qquad c(r,0) = 0, \quad r > 1, \tag{3.3}$$

representing an initially solute-free surrounding medium.

The extinction time follows from $S(t_e) = 0$, giving

$$t_e = \frac{1}{k^2}. \tag{3.4}$$

The planar approximation remains asymptotically valid as long as

$$\sqrt{t} \ll 1, \tag{3.5}$$

so that the diffusion layer remains thin relative to the particle radius.

3.2. Leading-order solution: diffusion-controlled regime

At leading order (Pe = 0), the concentration field is radially symmetric and admits the similarity form

$$c^{(0)}(r,t) = F(\xi). \tag{3.6}$$

Substitution into the diffusion equation under the planar approximation yields

$$F'' + \frac{\xi}{2}F' = 0, \qquad \xi > k, \tag{3.7}$$

with boundary conditions

$$F(k) = 1, \qquad F(\infty) = 0. \tag{3.8}$$

The unique bounded solution is

$$F(\xi) = \frac{\operatorname{erfc}(\xi/2)}{\operatorname{erfc}(k/2)}. \tag{3.9}$$

Its derivative at the interface is

$$F'(k) = -\frac{e^{-k^2/4}}{\sqrt{\pi}\,\operatorname{erfc}(k/2)}. \tag{3.10}$$

The Stefan condition at leading order, using (2.6), reads

$$-\frac{1}{\beta}\frac{dS}{dt} = \left.\frac{\partial c}{\partial r}\right|_{r=S}. \tag{3.11}$$

Using

$$\frac{\partial c}{\partial r} = -\frac{F'(\xi)}{\sqrt{t}},$$

and evaluating at $\xi = k$, we obtain

$$-\frac{1}{\beta}\left(-\frac{k}{2\sqrt{t}}\right) = -\frac{F'(k)}{\sqrt{t}},$$

which simplifies to

$$\frac{k}{2\beta} = -F'(k) = \frac{e^{-k^2/4}}{\sqrt{\pi}\,\operatorname{erfc}(k/2)}. \tag{3.12}$$

Equation (3.12) determines $k(\beta)$ uniquely. For increasing β, the parameter k increases monotonically, corresponding to a faster leading-order dissolution rate.

3.3. First-order correction: flow-induced anisotropy

At $O(\mathrm{Pe})$, advection breaks spherical symmetry. We write

$$c^{(1)}(r,\theta,t) = A(r,t)\cos\theta, \qquad A(r,t) = \sqrt{t}\,a(\xi). \tag{3.13}$$

The resulting similarity equation becomes

$$a'' + \frac{\xi}{2}a' = F'(\xi), \qquad \xi > k, \tag{3.14}$$

with

$$a(k) = 0, \qquad a(\infty) = 0. \tag{3.15}$$

This correction is antisymmetric with respect to the equatorial plane. The diffusion layer becomes thinner on the upstream side ($\theta = 0$) and thicker downstream ($\theta = \pi$), reflecting the directional influence of the imposed flow [6].

As β increases, the peak of $a(\xi)$ shifts to larger ξ while its magnitude decreases. This behavior reflects the increase of the leading-order gradient at the interface, which modifies the dipolar perturbation induced by advection.

3.4. Second-order isotropic correction

At $O(\mathrm{Pe}^2)$, the isotropic component is written as

$$c^{(2)}_{\mathrm{iso}}(r,t) = t\,b(\xi). \tag{3.16}$$

After spherical averaging, the governing equation reduces to

$$b'' + \frac{\xi}{2}b' = \frac{1}{3}a' + \frac{2}{3}\frac{a}{\xi}, \qquad \xi > k, \tag{3.17}$$

with

$$b(\infty) = 0. \tag{3.18}$$

Expanding the interface position as

$$S(t) = 1 - k\sqrt{t} + \mathrm{Pe}^2 S^{(2)}(t) + \cdots, \tag{3.19}$$

similarity consistency requires

$$S^{(2)}(t) = \sigma t^{3/2}. \tag{3.20}$$

Application of the Stefan condition at $O(\mathrm{Pe}^2)$ yields

$$\sigma = \frac{2}{3\beta}\,b'(k). \tag{3.21}$$

For the parameter values examined ($\beta = 0.2,\ 0.25,\ 0.3,\ 0.8$), we find $b'(k) > 0$, and therefore $\sigma > 0$, indicating that weak advection enhances the dissolution rate at second order in these cases.

3.5. Asymptotic structure and validity

Collecting all contributions, we obtain

$$S(t) = 1 - k\sqrt{t} + \mathrm{Pe}^2\,\sigma\, t^{3/2} + O(\mathrm{Pe}^3). \tag{3.22}$$

The neglected higher-order terms scale as $O(\mathrm{Pe}^3 t^2)$, consistent with the structure of the expansion. Hence, the truncation error remains negligible provided

$$\mathrm{Pe}^2 t \ll 1. \tag{3.23}$$

Within this regime, the asymptotic solution provides a uniformly valid approximation to the dissolution dynamics.

4. Results and discussion

The asymptotic solution derived in Section 3 provides a systematic description of how a weak uniform flow affects the dissolution of a spherical particle. In this section, we present the numerical results obtained by solving the similarity boundary-value problems (3.7)-(3.8), (3.14)-(3.15) and (3.17)-(3.18) together with condition (3.21). All computations are performed with the planar similarity variable $\xi = (1 - r)/\sqrt{t}$ and the interface law $S(t) = 1 - k\sqrt{t}$, where the constant $k > 0$ is determined from the transcendental equation (3.12). The numerical method uses a robust root-finding algorithm for k and a direct quadrature approach for the functions $a(\xi)$ and $b(\xi)$, ensuring high accuracy and stability even for large values of β.

4.1. Leading-order behaviour: diffusion-controlled dissolution

At leading order ($\mathrm{Pe} = 0$), the problem reduces to the classical diffusion-controlled dissolution of a spherical particle in a quiescent fluid. The concentration profile is given by the error-function solution (3.9), and the interface evolves as $S^{(0)}(t) = 1 - k\sqrt{t}$. The parameter k depends monotonically on the solubility ratio β through Eq (3.12). Table 1 lists the computed values of k for the four values of β examined.

Table 1. Leading-order constant $k(\beta)$ obtained from (3.12). Here, $\beta = (C_p - C_0)/(C_s - C_p)$ measures the inverse solubility contrast; smaller β corresponds to a larger driving force for dissolution.

β	0.2	0.25	0.3	0.8
k	0.259756	0.337998	0.423280	2.350433

As β increases, k grows monotonically; this reflects a faster leading-order dissolution rate when the solubility contrast is smaller (i.e., when β is larger). For $\beta = 0.8$, the value of k exceeds unity, indicating that the interface recedes more rapidly and the diffusion layer thickens accordingly. These results agree with the well-known planar Stefan solution [4, 12] and confirm the consistency of the present formulation in the absence of flow.

4.2. *First-order correction: dipolar anisotropy*

When advection is present, the spherical symmetry is broken. At $O(\mathrm{Pe})$, the concentration field acquires a dipolar correction of the form $c^{(1)} = \sqrt{t}\, a(\xi)\cos\theta$. Figure 1 displays the numerical solution of $a(\xi)$ for the four values of β. The profiles are antisymmetric about the equatorial plane and decay to zero as $\xi \to \infty$.

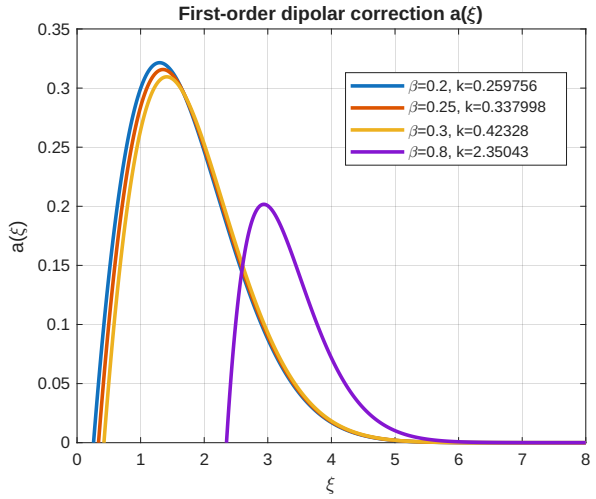

Figure 1. First-order dipolar correction $a(\xi)$ for different values of β.

Several features are noteworthy:

- **Shape and peak location:** Each profile rises from zero at the interface ($\xi = k$), reaches a maximum, and then decays monotonically. As β increases, the peak shifts to larger ξ and its magnitude decreases. For $\beta = 0.8$, the peak is barely visible and the correction remains very small over the entire domain. This behavior is a direct consequence of the increase of k: A larger interface position $\xi = k$ means that the diffusive layer extends further, and the relative influence of the flow on the already weak gradients is reduced.
- **Physical interpretation:** The dipolar correction makes the diffusion layer thinner on the upstream side ($\theta = 0$) and thicker downstream ($\theta = \pi$). Hence, the local flux is enhanced at the front and reduced at the rear, but the angular average of this correction vanishes identically. Consequently, the first-order correction to the interface position is $S^{(1)}(t) = 0$, as shown in Section 3.3. This cancellation is a key qualitative feature that distinguishes the moving-boundary problem from fixed-sphere heat/mass transfer analyses, where an $O(\mathrm{Pe})$ correction to the Nusselt number does appear.

4.3. *Second-order isotropic correction and the sign of σ*

At $O(\mathrm{Pe}^2)$, the nonlinear interaction between advection and the dipolar concentration field generates an isotropic component $c^{(2)}_{\mathrm{iso}}(r,t) = t\, b(\xi)$ that survives spherical averaging. Figure 2 shows the numerical solution of $b(\xi)$ for the same values of β.

The slope at the interface, $b'(k)$, determines the constant σ through relation (3.21), i.e., $\sigma = \frac{2}{3\beta} b'(k)$. The computed values are summarized in Table 2.

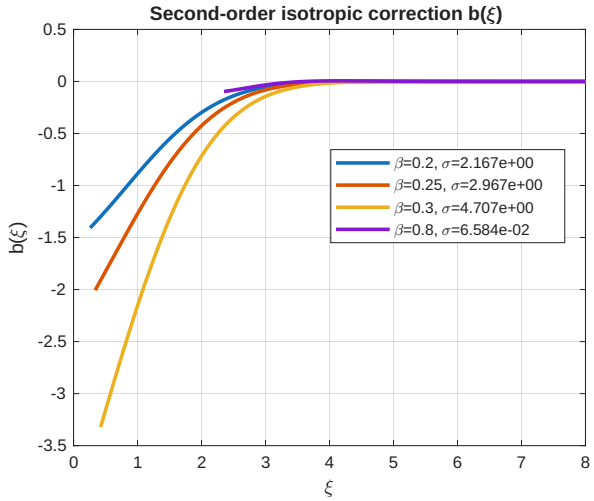

Figure 2. Second-order isotropic correction $b(\xi)$ for different values of β .

Table 2. Second-order coefficient $\sigma(\beta)$ obtained from (3.21).

β	0.2	0.25	0.3	0.8
σ	2.167	2.967	4.707	0.06584

For $\beta = 0.2,\ 0.25,\ 0.3$, we find σ of order unity, while for $\beta = 0.8$, it drops to 0.066. In all cases $\sigma > 0$, indicating that the second-order correction $\mathrm{Pe}^2\sigma t^{3/2}$ adds to the leading-order term $1 - k\sqrt{t}$; consequently, the particle shrinks faster than in the purely diffusive situation. Thus, within the range of parameters studied, weak advection accelerates the dissolution process at second order.

The decrease of σ with increasing β is physically plausible: When the solubility contrast is small (large β), the leading-order concentration gradients are weaker, and the nonlinear mechanism that produces the isotropic correction becomes less effective. For $\beta = 0.8$, the correction is more than one order of magnitude smaller than for $\beta = 0.2$, showing that the flow effect is most pronounced when diffusion is strong (small β).

4.4. Asymptotic dissolution law and regime of validity

Collecting the contributions from each order, the particle radius evolves according to

$$S(t) = 1 - k\sqrt{t} + \mathrm{Pe}^2\,\sigma\,t^{3/2} + O(\mathrm{Pe}^3). \tag{4.1}$$

The neglected terms scale as $O(\mathrm{Pe}^3 t^2)$; therefore, the expansion remains uniformly valid as long as

$$\mathrm{Pe}^2 t \ll 1. \tag{4.2}$$

Condition (4.2) defines the time window over which the asymptotic approximation is reliable. For a given Péclet number, it restricts the analysis to times satisfying $t \ll \mathrm{Pe}^{-2}$. In practice, this covers the early and intermediate stages of dissolution; for longer times or larger Péclet numbers, higher-order corrections would become significant, and a rescaled analysis or full numerical simulation would be required.

4.5. Discussion and physical interpretation

The results presented above lead to several important conclusions:

- **Vanishing of the first-order interface correction:** Although the flow distorts the concentration field at $O(\mathrm{Pe})$, its dipolar symmetry implies that the angular average of the corresponding flux contribution vanishes. Hence, the mean dissolution rate is unchanged at this order. This cancellation is robust and is expected to persist under more realistic low-Reynolds-number flow disturbances, since the leading correction retains the same dipolar symmetry.
- **Nonlinear origin of flow-enhanced dissolution:** The first non-zero modification of the interface motion appears at $O(\mathrm{Pe}^2)$ and is governed by an isotropic concentration component. For the parameter values examined, the computed coefficient σ is positive, indicating that weak advection accelerates dissolution at second order.
- **Dependence on β:** As β increases (i.e., the concentration jump $C_s - C_p$ becomes smaller relative to $C_p - C_0$), the leading-order constant k increases, the peak of $a(\xi)$ shifts to larger ξ with reduced magnitude, and the magnitude of σ decreases markedly. These trends are consistent with the physical expectation that the influence of flow weakens when the diffusive driving gradients are milder.

5. Conclusions

A mathematical analysis has been presented for the dissolution of a spherical particle subjected to an imposed uniform flow. The problem was formulated as a free-boundary problem governed by an advection-diffusion equation in the exterior of the particle, coupled with a Stefan condition at the moving interface. An asymptotic expansion in the Péclet number, $\mathrm{Pe} = US_0/D$, was employed to examine the influence of a weak flow on the dissolution kinetics in a systematic manner. The analysis focuses on the early stages of dissolution, where the diffusion length remains small compared to the initial particle radius, allowing a planar approximation of the concentration boundary layer.

The principal findings are as follows:

- **Consistent formulation:** By adopting the planar similarity variable $\xi = (1 - r)/\sqrt{t}$ and the interface law $S(t) = 1 - k\sqrt{t}$ with $k > 0$, the classical Stefan condition is recast in a form that naturally yields a shrinking radius and avoids any sign ambiguity. The dimensionless parameter $\beta = (C_p - C_0)/(C_s - C_p)$ quantifies the inverse solubility contrast; smaller β corresponds to a larger driving force for dissolution.
- **Leading-order behaviour:** At $\mathrm{Pe} = 0$, the problem reduces to the classical diffusion-controlled dissolution of a sphere, with the concentration profile given by the error-function solution $F(\xi) = \operatorname{erfc}(\xi/2)/\operatorname{erfc}(k/2)$. The constant k is determined from the transcendental equation

$$\frac{k}{2\beta} = \frac{e^{-k^2/4}}{\sqrt{\pi}\,\operatorname{erfc}(k/2)}.$$

  Numerical values of k for $\beta = 0.2, 0.25, 0.3, 0.8$ are reported in Table 1; they increase monotonically with β, reflecting faster leading-order dissolution when the solubility contrast is smaller.

- **First-order flow effect dipolar anisotropy:** At $O(\mathrm{Pe})$, the uniform flow generates a dipolar correction $c^{(1)} = \sqrt{t}\, a(\xi)\cos\theta$. The function $a(\xi)$, obtained from a linear boundary-value problem, is antisymmetric about the equatorial plane and decays to zero as $\xi \to \infty$. This correction steepens the concentration gradient on the upstream side and flattens it downstream, but its angular average vanishes exactly. Consequently, the mean interfacial flux, and hence the interface position, receives no correction at this order: $S^{(1)}(t) = 0$.
- **Second-order flow effect isotropic enhancement:** The first non-zero modification of the dissolution rate appears at $O(\mathrm{Pe}^2)$. Nonlinear interaction between advection and the dipolar field produces an isotropic component $c^{(2)}_{\mathrm{iso}} = t\, b(\xi)$. Solving the corresponding boundary-value problem with condition (3.21) yields $b(\xi)$ and its interfacial slope $b'(k)$. The second-order correction to the interface is $S^{(2)}(t) = \sigma t^{3/2}$ with $\sigma = \frac{2}{3\beta} b'(k)$. For all cases examined, $\sigma > 0$, indicating that weak advection accelerates dissolution. The computed values (Table 2) show that σ decreases as β increases; for $\beta = 0.8$, it is more than one order of magnitude smaller than for $\beta = 0.2$, confirming that the flow effect is most pronounced when the diffusive driving force is strong (small β).
- **Asymptotic dissolution law and validity:** Collecting all contributions, the particle radius evolves according to

$$S(t) = 1 - k\sqrt{t} + \mathrm{Pe}^2\, \sigma\, t^{3/2} + O(\mathrm{Pe}^3).$$

  The expansion remains uniformly valid as long as $\mathrm{Pe}^2 t \ll 1$, i.e., for times $t \ll \mathrm{Pe}^{-2}$. This condition defines the regime in which the asymptotic approximation is quantitatively reliable.

The analysis provides a mathematically consistent extension of classical diffusion-controlled dissolution models to incorporate weak advective transport. It demonstrates that the influence of a uniform flow on the dissolution rate is intrinsically a second-order effect, arising from nonlinear interactions rather than linear superposition. The dipolar symmetry of the first-order concentration field and the consequent vanishing of its angular average are robust features that would persist even with a more realistic Stokes-flow disturbance, because the leading velocity perturbation retains the same symmetry.

The formulation clarifies the sign convention, time-scale definition, and regime of validity, and provides complete second-order asymptotic results together with their physical interpretation. The angular asymmetry induced by the flow is discussed in detail, and the influence of the parameter β on the solution is explained.

Several extensions of this work merit consideration. The assumption of a spatially uniform, prescribed velocity field could be refined by coupling the dissolution problem with a more realistic flow, such as Stokes flow past a sphere; the qualitative conclusion that the first interface correction arises at $O(\mathrm{Pe}^2)$ is expected to persist. Extension to larger Péclet numbers would require a rescaled analysis or direct numerical simulation of the full advection-diffusion equation. Finally, the methodology can be adapted to other flow configurations (e.g., shear flow, oscillatory flow) and to non-spherical particle geometries, offering a systematic route to quantify flow effects in a wide range of dissolution problems.

Use of Generative-AI tools declaration

The author declares she has not used Artificial Intelligence (AI) tools in the creation of this article.

Conflict of interest

The author declares no conflict of interest.

References

1. A. Friedman, *Variational principles and free-boundary problems*, New York: John Wiley & Sons, 1982.
2. J. Crank, *The mathematics of diffusion*, 2 Eds., Oxford: Oxford University Press, 1975.
3. L. I. Rubinstein, *The Stefan problem*, American Mathematical Society, 1971.
4. H. S. Carslaw, J. C. Jaeger, *Conduction of heat in solids*, 2 Eds., Oxford: Clarendon Press, 1959.
5. A. Alhowaity, Dissolution of a spherical particle with a moving boundary in a flow field, *Int. J. Modern Phys. B*, **38** (2024), 2450002. https://doi.org/10.1142/S0217979224500024
6. R. B. Bird, W. E. Stewart, E. N. Lightfoot, *Transport phenomena*, 2 Eds., John Wiley & Sons, 2007.
7. C. M. Bender, S. A. Orszag, *Advanced mathematical methods for scientists and engineers*, McGraw-Hill, 1978.
8. D. Thenmozhi, M. E. Rao, R. R. Devi, C. Nagalakshmi, P. Selvi, Dynamics of heat transfer in complex fluid systems: comparative analysis of Jeffrey, Williamson and Maxwell fluids with chemical reactions and mixed convection, *Int. J. Thermofluids*, **24** (2024), 100896. https://doi.org/10.1016/j.ijft.2024.100896
9. R. Hajlaoui, A. Abbas, F. Anwar, M. M. Boudabous, A. Chabir, W. Hassen, et al., Magnetohydrodynamic Maxwell hybrid nanofluid flow and heat transfer over a moving needle in porous media, *Sci. Rep.*, **15** (2025), 19194. https://doi.org/10.1038/s41598-025-04071-8
10. M. Bilal, M. Sagheer, S. Hussain, On MHD 3D upper convected Maxwell fluid flow with thermophoretic effect using nonlinear radiative heat flux, *Can. J. Phys.*, **96** (2018), 1–10. https://doi.org/10.1139/cjp-2017-0250
11. L. G. Leal, *Advanced transport phenomena: fluid mechanics and convective transport processes*, Cambridge University Press, 2007.
12. S. Howison, *Practical applied mathematics: modelling, analysis, approximation*, Cambridge University Press, 2005.

AIMS Press